Applied Acoustics 73 (2012) 356–365

Contents lists available at SciVerse ScienceDirect

Applied Acoustics

journal homepage: www.elsevier.com/locate/apacoust

Free vibrations of a generally restrained rectangular plate with an internal line hinge

María Virginia Quintana *, Ricardo Oscar Grossi [1]

INIQUI-PROMAS, Facultad de Ingeniería, Universidad Nacional de Salta, Av. Bolivia 5150, 4400 Salta, Argentina

A R T I C L E I N F O

Article history:
Received 11 May 2011
Received in revised form 20 October 2011
Accepted 27 October 2011
Available online 23 November 2011

Keywords:
Vibrations
Plates
Internal line hinge
Lagrange multipliers
Elastic restraints

A B S T R A C T

This paper deals with the study of free transverse vibrations of rectangular plates with an internal line hinge and elastically restrained boundaries. The equations of motion and its associated boundary and transition conditions are rigorously derived using Hamilton's principle. The governing eigenvalue equation is solved employing a combination of the Ritz method and the Lagrange multipliers method. The deflections of the plate and the Lagrange multipliers are approximated by polynomials as coordinate functions. The developed algorithm allows obtaining approximate solutions for plates with different aspect ratios, boundary conditions, including edges elastically restrained by both translational and rotational springs, and arbitrary locations of the line hinge. Therefore, a unified algorithm has been implemented. Sets of parametric studies are performed and the results are given in graphical and tabular form.

1. Introduction

The plate is probably one of the most common structural element that has been devised by either scientific or technological interest. It is widely encountered in aerospace, marine, mechanical and civil engineering structures. The dynamical behavior of plates is one of the major concerns in designing this type of structures. Vibration characteristics of plates have been extensively studied over the last 100 years. It is not the intention to review the literature consequently, some of the relevant papers will be cited. Plates with different shapes, boundary conditions and complicating effects have been considered and the frequency parameters were documented in monographs [1,2], standard texts [3–5] and review papers [6,7].

Several complicating effects have been considered such as: elastically restrained boundaries, presence of elastically or rigidly connected masses, variable thickness, anisotropic material, and presence of holes. In Refs. [8–11] general studies on vibration of plates with point supports have been presented and vibration of plates with line supports have been developed in Refs. [12–14]. A review of the literature has shown that there is only a limited amount of information for the vibration of plates with line hinges. A line hinge in a plate can be used to facilitate folding of gates or the opening of doors among other applications. The hinge can also be used to simulate a through crack along the interior of the plate. Xiang and Reddy [15] provided the first-known solutions based on the first order shear deformation theory for vibration of rectangular plates with an internal line hinge. The Lévy method and the state-space technique were employed to solve the vibration problem. However, the method can only be applied to a rectangular plate with at least two parallel edges simply supported. More recently, Huang et al. [16] developed a discrete method for analyzing the free vibration problem of thin and moderately thick rectangular plates with a line hinge and various classical boundary conditions. Lin et al. [17] derived and used an analytical solution for studying the effect of off-neutral axis loading (point force excitation applied off the neutral axis of a rib) on ribbed-plate responses. It must be noted that the analytical approach could be employed to predict the free vibration of plates with hinges.

Often, the restraints along the boundaries of a real system cannot be actually represented by classical edge conditions such as simply supported, clamped and free. Therefore, it is of great importance to study the vibration characteristics of elastically restrained plates. However, the general problem of free vibration of plates with internal line hinges and with edges elastically restrained against rotation and translation has not been treated so, the aim of this paper, is to provide an approximate analytical solution to this problem based on the classical Kirchhoff plate theory.

Stimulated by the development of the study of the mentioned plate problems, interest in variational methods has grown in recent decades. The Ritz method has gained considerable popularity, being used by engineers and scientists as a very effective tool. When applying this method it is necessary to select a sequence of functions, called coordinate functions. The solution of the variational problem is then approximated by a linear combination of these functions. In fact, the most critical feature of the Ritz method

* Corresponding author.
E-mail address: virginiaquintana@argentina.com (M.V. Quintana).
[1] Research Member of CONICET.

0003-682X/$ - see front matter © 2011 Elsevier Ltd. All rights reserved.
doi:10.1016/j.apacoust.2011.10.010

is regarding the choice of the coordinate functions. When the Ritz method is applied to a structure obtained by joining several components together, the transition conditions require the continuity of displacement between all the junctions of the structural components. These transition conditions give rise to several problems in the rational choice of the coordinate functions. Fortunately it is not necessary to subject the coordinate functions to the natural boundary conditions [18,19]. This is particularly true in the case of a plate with an internal line hinge. For this reason in this paper only the essential transition condition along the line hinge,is taken into account with the Lagrange multipliers [20–22]. The developed methodology is based on the Ritz method where the transverse deflections and the Lagrange multiplier are approached by sets of simple polynomials expressions.

To demonstrate the validity and efficiency of the proposed algorithm, results of a convergence study are included, several numerical examples not previously treated are presented and some particular cases are compared with results presented by other authors. Sets of parametric studies are performed and the results are given in graphical and tabular form. Also, in the present paper, a complete rigorous application of the Hamilton's principle is developed for the derivation of equations of motion and its associated boundary and transition conditions.

2. The determination of the boundary value problem

Let us consider an isotropic rectangular thin plate of variable thickness h, length a and width b. An internal line hinge that is parallel to the y-axis is located at $x = c$, as shown in Fig. 1. The whole domain of the plate A is considered to have two sub domains $A^{(1)}$ and $A^{(2)}$ which correspond respectively to the left and the right part of the plate and are separated by the line $\Gamma^{(c)}$. We assume that different rigidities $D^{(i)}$ and mass density $\rho h^{(i)}$ of the isotropic material, correspond to the sub domains $A^{(1)}$ and $A^{(2)}$.The rotational restraints are characterized by the functions $c_r^{(i)}(s)$ and the translational restraints by the functions $c_t^{(i)}(s)$, where s denotes the arc length measured from the point $P^{(i)}$ of the boundary $\partial A^{(i)}$ (see Fig. 1).

As usual, in order to analyze the transverse displacements of the system under study we suppose that the vertical position of the plate at any time t, is described by the function $w = w(x,y,t)$, where $(x,y) \in \bar{A}$ and $\bar{A} = A \cup \partial A$. At time t, the kinetic energy of the plate is given by

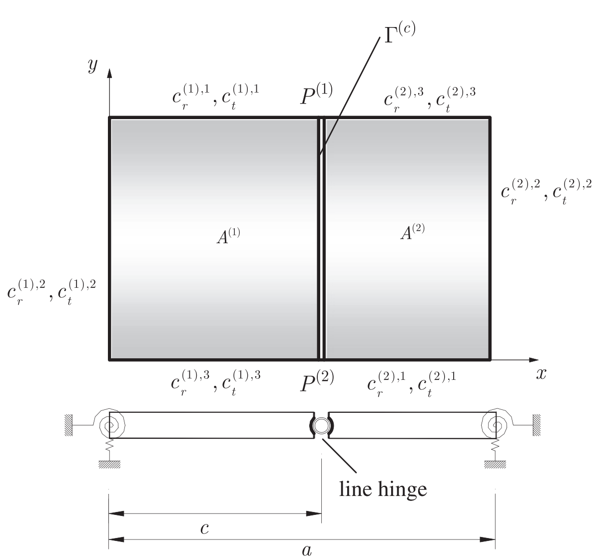

Fig. 1. General description of the mechanical system under study.

$$E_K(w) = \frac{1}{2}\sum_{i=1}^{2}\int\int_{A^{(i)}} \rho h^{(i)} \left(\frac{\partial w}{\partial t}\right)^2 dx\,dy, \quad (1)$$

where $h^{(i)} = h^{(i)}(x,y)$ and

$$w(x,y,t) = \begin{cases} w^{(1)}(x,y,t), \forall (x,y) \in \bar{A}^{(1)}, \\ w^{(2)}(x,y,t), \forall (x,y) \in \bar{A}^{(2)}, \end{cases} \quad (2)$$

Hence $w^{(i)}$ is the restriction of the function w to $\bar{A}^{(i)}$.

At time t, the total potential energy due to the elastic deformation of the plate deformed by an external load $q = q(x,y,t)$ acting on $\bar{A}$, and to the deformation of the elastic restraints on the boundary ∂A, is given by:

$$E_D(w) = \frac{1}{2}\sum_{i=1}^{2}\left\{\int\int_{A^{(i)}}\left[D^{(i)}\left(\left(\frac{\partial^2 w}{\partial x^2}+\frac{\partial^2 w}{\partial y^2}\right)^2 -2(1-\mu)\left(\frac{\partial^2 w}{\partial x^2}\frac{\partial^2 w}{\partial y^2}-\left(\frac{\partial^2 w}{\partial x^2 \partial y^2}\right)^2\right)\right) - 2q^{(i)}w\right]dx\,dy + \int_{\Gamma^{(i)}} c_r^{(i)}(x,y)w^2(x,y,t)ds + \int_{\Gamma^{(i)}} c_t^{(i)}(x,y)\left(\frac{\partial w}{\partial n}(x,y,t)\right)^2 ds\right\}, \quad (3)$$

where w is given by Eq. (2), i.e. $w = w^{(i)}$, $\forall (x,y) \in A^{(i)}$ and the functions $q^{(i)}$ are defined in the same form as the functions $w^{(i)}$ in Eq. (2). Based on Eq. (2) $w^{(i)}$ is replaced by w in Eqs. (1) and (3). Hence, $\partial w/\partial n$ denotes the directional derivate of $w^{(i)}$ with respect to the outward normal unit vector to the curve $\Gamma^{(i)} = \partial A^{(i)} - \Gamma^{(c)}$, $i = 1, 2$.

Hamilton's principle requires that between times t_0 and t_1, at which the positions of the mechanical system are known, it should execute a motion which makes stationary the functional $F(w) = \int_{t_0}^{t_1}(E_K - E_D)dt$, on the space of admissible functions. This leads to

$$F(w) = \frac{1}{2}\int_{t_0}^{t_1}\left\{\sum_{i=1}^{2}\left[\int\int_{A^{(i)}}\left(\rho h^{(i)}\left(\frac{\partial w}{\partial t}\right)^2 - D^{(i)}\left(\left(\frac{\partial^2 w}{\partial x^2}+\frac{\partial^2 w}{\partial y^2}\right)^2 -2(1-\mu)\left(\frac{\partial^2 w}{\partial x^2}\frac{\partial^2 w}{\partial y^2}\left(\frac{\partial^2 w}{\partial x^2 \partial y^2}\right)^2\right)\right)+2q^{(i)}w\right)dx\,dy\right] - U_R - U_T\right\}dt, \quad (4)$$

where (see Fig. 1)

$$U_R = \int_0^c c_r^{(1),1}(x,b)\left(\frac{\partial w^{(1)}}{\partial y}\right)^2(x,b,t)dx + \int_0^b c_r^{(1),2}(0,y)\left(\frac{\partial w^{(1)}}{\partial x}\right)^2(0,y,t)dy + \int_0^c c_r^{(1),3}(x,0)\left(\frac{\partial w^{(1)}}{\partial y}\right)^2(x,0,t)dx + \int_c^a c_r^{(2),1}(x,0)\left(\frac{\partial w^{(2)}}{\partial y}\right)^2(x,0,t)dx + \int_0^b c_r^{(2),2}(a,y)\left(\frac{\partial w^{(2)}}{\partial x}\right)^2(a,y,t)dy + \int_c^a c_r^{(2),3}(x,b)\left(\frac{\partial w^{(2)}}{\partial y}\right)^2(x,b,t)dx. \quad (5)$$

The expression of U_T is obtained from Eq. (5) by replacing $c_r^{(i),j}$ by $c_t^{(i),j}$ and the derivatives by the corresponding functions.

The definition of the variation of F at w in the direction v, is given as a generalization of the definition of the directional derivative of a real valued function defined on a subset of $\mathbb{R}^n$ [23]. Consequently, the definition of the first variation of F at w in the direction v, is given by

$$\delta F(w;v)=\frac{dF}{d\varepsilon}(w+\varepsilon v)\bigg|_{\varepsilon=0}. \tag{6}$$

The condition of stationary functional requires that

$$\delta F(w;v)=0, \forall v\in D_v, \tag{7}$$

where $\delta F(w;v)$ is the first variation of F at w in the direction v and D_v is the space of admissible directions at w for the domain D_w of this functional.

In order to make the mathematical developments required by the application of the techniques of the calculus of variations, we assume that:

$$h^{(i)}\in C\overline{A}^{(i)}), q^{(i)}(\cdot,\cdot,t)\in C(\overline{A}^{(i)}), D^{(i)}\in C^2(\overline{A}^{(i)}), w(x,y,\cdot)\in C^2[t_0,t_1], w(\cdot,\cdot,t)\in C(\overline{A}), \text{and} w(\cdot,\cdot,t)|_{\overline{A}^{(i)}}\in C^4(\overline{A}^{(i)}),$$
$$\overline{A}^{(i)}=A^{(i)}\cup\partial A^{(i)}, i=1,2.$$

It must be noted that as a consequence of the presence of the line hinge the derivative $\partial w/\partial x$ is not continuous and the classical derivatives $\partial^2 w/\partial x^2$, $\partial^2 w/\partial x\partial y,\ldots$ do not necessarily exist in the domain A, so it is necessary to impose the conditions

$$w(\cdot,\cdot,t)|_{\overline{A}^{(i)}}\in C^4(\overline{A}^{(i)}), i=1,2.$$

In view of all these observations and since Hamilton's principle requires that at times t_0 and t_1 the positions are known, the space D_w is given by

$$D_w=\Big\{w; w(x,y,\cdot)\in C^2[t_0,t_1], w(\cdot,\cdot,t)\in C(\overline{A}), w(\cdot,\cdot,t)|_{\overline{A}^{(i)}}\in C^4(\overline{A}^{(i)}), = 1,2, w(x,y,t_0), w(x,y,t_1) \text{ prescribed}\}. \tag{8}$$

The only admissible directions v at $w\in D_w$ are those for which $w+\varepsilon v\in D_w$ for all sufficiently small ε and $\delta F(w;v)$ exists. In consequence, and in view of Eq. (8), v is an admissible direction at w for D_w if, and only if, $v\in D_v$ where

$$D_v=\Big\{v; v(x,y,\cdot)\in C^2[t_0,t_1], v(\cdot,\cdot,t)\in C(\overline{A}), v(\cdot,\cdot,t)|_{\overline{A}^{(i)}}\in C^4(\overline{A}^{(i)}), i=1,2,\ v(x,y,t_0t)=v(x,y,t_1)=0, \forall(x,y)\in\overline{A}\Big\}. \tag{9}$$

Performing the derivative (6) with F given by Eq. (4), we have

$$\delta F(w;v)=\int_{t_0}^{t_1}\Bigg\{\sum_{i=1}^{2}\Bigg[\int\int_{A^{(i)}}\Bigg(\rho h^{(i)}\frac{\partial w}{\partial t}\frac{\partial v}{\partial t}-D^{(i)}\left(\frac{\partial^2 w}{\partial x^2}\frac{\partial^2 v}{\partial x^2}+\frac{\partial^2 w}{\partial y^2}\frac{\partial^2 v}{\partial y^2}\right) -\mu D^{(i)}\left(\frac{\partial^2 w}{\partial x^2}\frac{\partial^2 v}{\partial y^2}+\frac{\partial^2 w}{\partial y^2}\frac{\partial^2 v}{\partial x^2}\right)-2D^{(i)}(1-\mu)\left(\frac{\partial^2 w}{\partial x\partial y}\frac{\partial}{\partial x}\left(\frac{\partial v}{\partial y}\right) +\frac{\partial^2 w}{\partial y\partial x}\frac{\partial}{\partial y}\left(\frac{\partial v}{\partial x}\right)\right)+q^{(i)}v\Bigg)dxdy-VU_R-VU_T\Bigg\}dt, \tag{10}$$

where:

$$\begin{aligned}VU_R=&\int_0^c c_r^{(1),1}(x,b)\left(\frac{\partial w^{(1)}}{\partial y}\frac{\partial v^{(1)}}{\partial y}\right)(x,b,t)dx\\
&+\int_0^b c_r^{(1),2}(0,y)\left(\frac{\partial w^{(1)}}{\partial x}\frac{\partial v^{(1)}}{\partial x}\right)(0,y,t)dy\\
&+\int_0^c c_r^{(1),3}(x,0)\left(\frac{\partial w^{(1)}}{\partial y}\frac{\partial v^{(1)}}{\partial y}\right)(x,0,t)dx\\
&+\int_c^a c_r^{(2),1}(x,0)\left(\frac{\partial w^{(2)}}{\partial y}\frac{\partial v^{(2)}}{\partial y}\right)(x,0,t)dx\\
&+\int_0^b c_r^{(2),2}(a,y)\left(\frac{\partial w^{(2)}}{\partial x}\frac{\partial v^{(2)}}{\partial x}\right)(a,y,t)dy\\
&+\int_c^a c_r^{(2),3}(x,b)\left(\frac{\partial w^{(2)}}{\partial y}\frac{\partial v^{(2)}}{\partial y}\right)(x,b,t)dx.\end{aligned} \tag{11}$$

The expression of VU_T is obtained from Eq. (11) by replacing $c_r^{(i),j}$ by $c_t^{(i),j}$ and the derivatives by the corresponding functions.

Let us consider the first term of Eq. (10). Since $w(x,y,\cdot)$, $v(x,y,\cdot)\in C^2[t_0,t_1]$ we can integrate by parts with respect to t and if we apply the conditions $v(x,y,t_0)=v(x,y,t_1)=0, \forall(x,y)\in\overline{A}$, imposed in Eq. (9), we obtain

$$\int_{t_0}^{t_1}\int\int_{A^{(i)}}\rho h^{(i)}\frac{\partial w}{\partial t}\frac{\partial v}{\partial t}dx\,dy\,dt=-\int_{t_0}^{t_1}\int\int_{A^{(i)}}\rho h^{(i)}\times\frac{\partial^2 w}{\partial t^2}v\,dx\,dy\,dt. \tag{12}$$

To transform the terms of Eq. (10) which are multiplied by the coefficient $D^{(i)}$, we employ the well known Green's formula:

$$\int_G u(x)\frac{\partial v(x)}{\partial x_j}dx=\int_{\partial G}u(x)v(x)n_j(x)ds-\int_G v(x)\frac{\partial u(x)}{\partial x_j}dx,\quad j=1,2,\ u,v\in C^{(1)}(\overline{G}), \tag{13}$$

where $x=(x_1,x_2)$ and n_j denotes the jth component of the outward unit normal to the boundary ∂G. We have, upon applying twice Eq. (13) and using Eq. (12) that:

$$\delta F(w;v)=\int_{t_0}^{t_1}\Bigg\{\sum_{i=1}^{2}\Bigg[\int\int_{A^{(i)}}\Bigg(-\rho h^{(i)}\frac{\partial^2 w}{\partial t^2}+\frac{\partial^2 M_1^{(i)}}{\partial x^2}+\frac{\partial^2 M_2^{(i)}}{\partial y^2} +2\frac{\partial^2 H_{12}^{(i)}}{\partial x\partial y}+q^{(i)}\Bigg)v\,dxdy+\int_{\partial A^{(i)}}M_{12}^{(i)}ds -\int_{\partial A^{(i)}}\left(\sum_{j=1}^{2}N_j^{(i)}n_j^{(i)}\right)v\,ds-VU_R-VU_T\Bigg\}dt, \tag{14}$$

where

$$M_1^{(i)}=-D^{(i)}\left(\frac{\partial^2 w}{\partial x^2}+\mu\frac{\partial^2 w}{\partial y^2}\right), M_2^{(i)}=-D^{(i)}\left(\frac{\partial^2 w}{\partial y^2}+\mu\frac{\partial^2 w}{\partial x^2}\right), \tag{15a, b}$$

$$H_{12}^{(i)}=-(1-\mu)D^{(i)}\left(\frac{\partial^2 w}{\partial x\partial y}\right), N_1^{(i)}=\frac{\partial M_1^{(i)}}{\partial x}+\frac{\partial H_{12}^{(i)}}{\partial y},\quad N_2^{(i)}=\frac{\partial M_2^{(i)}}{\partial y}+\frac{\partial H_{12}^{(i)}}{\partial x}, \tag{16a, b, c}$$

$$M_{12}^{(i)}=M_1^{(i)}\frac{\partial v}{\partial x}n_1^{(i)}+M_2^{(i)}\frac{\partial v}{\partial y}n_2^{(i)}+H_{12}^{(i)}\left(\frac{\partial v}{\partial x}n_2^{(i)}+\frac{\partial v}{\partial y}n_1^{(i)}\right). \tag{17}$$

According to the condition of stationary functional given by Eq. (7), the Eq. (14) must vanish for the function w corresponding to the actual motion of the plate for all admissible directions v, and in particular for all admissible $v^{(i)}$(the restriction of v to $A^{(i)}$), satisfying on the whole contours $\partial A^{(i)}$ the conditions:

$$v(x,y,t)|_{\partial A^{(i)}}=0, \frac{\partial v}{\partial x}(x,y,t)\bigg|_{\partial A^{(i)}}=0, \frac{\partial v}{\partial y}(x,y,t)\bigg|_{\partial A^{(i)}}=0,\quad i=1,2. \tag{18a, b, c}$$

In this case, the curvilinear integrals and the one-dimensional definite integrals in Eq. (14) vanish, and only the double integrals remain:

$$\delta F(w;v)=\int_{t_0}^{t_1}\Bigg[\sum_{i=1}^{2}\int\int_{A^{(i)}}\times\left(-\rho h^{(i)}\frac{\partial^2 w}{\partial t^2}+\frac{\partial^2 M_1^{(i)}}{\partial x^2}+\frac{\partial^2 M_2^{(i)}}{\partial y^2}+2\frac{\partial^2 H_{12}^{(i)}}{\partial x\partial y}+q^{(i)}\right)v\,dxdy\Bigg]dt. \tag{19}$$

Since v is an arbitrary smooth function satisfying the Eq. (18), we have from the fundamental lemma of the calculus of variations, that the restrictions $w^{(i)}$of the function w to $A^{(i)}$ must respectively satisfy the following differential equations

$$\frac{\partial^2}{\partial x^2}\left(D^{(i)}\frac{\partial^2 w^{(i)}}{\partial x^2}+\mu D^{(i)}\frac{\partial^2 w^{(i)}}{\partial y^2}\right)+\frac{\partial^2}{\partial y^2}\left(\mu D^{(i)}\frac{\partial^2 w^{(i)}}{\partial x^2}+D^{(i)}\frac{\partial^2 w^{(i)}}{\partial y^2}\right)$$
$$+2(1-\mu)\frac{\partial^2}{\partial x\partial y}\left(D^{(i)}\frac{\partial^2 w^{(i)}}{\partial x\partial y}\right)+\rho h^{(i)}\frac{\partial^2 w^{(i)}}{\partial t^2}-q^{(i)}=0,$$
$$\forall(x,y)\in A^{(i)},\quad i=1,2,\forall t\geqslant 0. \tag{20}$$

The fourth order partial differential equations given by Eq. (20) describe the dynamical behavior of the vibrating plate. If we set $q\equiv 0$, so that there is no external forces acting on the plate, the Eq. (20) reduce to the equations of free vibrations of the anisotropic plate. If we set $\partial^2 w/\partial t^2\equiv 0$, and it is assumed that all variables are independent of time, the Eq. (20) reduce to the equations which describe the statical behavior of the mentioned plate when a load of density $q = q(x,y)$ is applied on $\bar{A}$. Next, we remove the Eq. (18) and since the functions $w^{(i)}, i = 1, 2$, must satisfy the Eq. (20), the Eq. (14) reduces to

$$\delta F(w;v)=\int_{t_0}^{t_1}\left\{\sum_{i=1}^{2}\left[\int_{\partial A^{(i)}}M_{12}^{(i)}(x,y,t)ds\right.\right.$$
$$\left.\left.-\int_{\partial A^{(i)}}\left(\sum_{j=1}^{2}N_j^{(i)}(x,y,t)n_j^{(i)}(x,y)\right)v(x,y,t)ds-VU_R-VU_T\right\}dt. \tag{21}$$

Since we can independently choose v and its derivatives and the interval $[t_0,t_1]$ is arbitrary, the condition of stationary functional given by Eq. (6) applied to Eq. (21), leads in the manner for achieving Eq. (20), to the following boundary conditions:

$$c_r^{(1),1}(x,b)\frac{\partial w^{(1)}}{\partial y}(x,b,t)$$
$$=-\left(D^{(1)}(x,b)\frac{\partial^2 w^{(1)}}{\partial y^2}(x,b,t)+\mu D^{(1)}(x,b)\frac{\partial^2 w^{(1)}}{\partial x^2}(x,b,t)\right),x\in[0,c]. \tag{22}$$

$$c_t^{(1),1}(x,b)w(x,b,t)$$
$$=\frac{\partial}{\partial y}\left(D^{(1)}(x,b)\left(\frac{\partial^2 w^{(1)}}{\partial y^2}(x,b,t)+\mu\frac{\partial^2 w^{(1)}}{\partial x^2}(x,b,t)\right)\right)$$
$$+2(1-\mu)\frac{\partial}{\partial x}\left(D^{(1)}(x,b)\frac{\partial^2 w^{(1)}}{\partial x\partial y}(x,b,t)\right),x\in[0,c]. \tag{23}$$

Operating in a similar fashion we get the remaining boundary conditions and also those which correspond to the domain $A^{(2)}$.

3. The transition conditions

Since the domain of definition of the problem is the open set $A\subset\mathbb{R}^2$, all the points of the line $\Gamma^{(c)}$ are interior points of A and the equations formulated on it are not boundary conditions hence, they can be called *transition conditions*.

When $\Gamma^{(c)}$ is considered as part of $A^{(1)}$ the components of the outward unit normal are given by $n_1 = 1, n_2 = 0$. Hence from Eq. (21) it is immediate that the corresponding curvilinear integral is given by

$$\int_{\Gamma^{(c)}}\left(M_1^{(1)}\frac{\partial v}{\partial x}+H_{12}^{(1)}\frac{\partial v}{\partial y}-N_1^{(1)}v\right)ds. \tag{24}$$

Eq. (24) and the corresponding curvilinear integral when $\Gamma^{(c)}$ is considered as a part of $\partial A^{(2)}$, lead to the following transition conditions:

$$D^{(1)}(c,y)\frac{\partial^2 w^{(1)}}{\partial x^2}(c,y,t)+\mu D^{(1)}(c,y)\frac{\partial^2 w^{(1)}}{\partial y^2}(c,y,t)=0,\forall y\in[0,b], \tag{25}$$

$$D^{(2)}(c,y)\frac{\partial^2 w^{(2)}}{\partial x^2}(c,y,t)+\mu D^{(2)}(c,y)\frac{\partial^2 w^{(2)}}{\partial y^2}(c,y,t)=0,\forall y\in[0,b]. \tag{26}$$

$$\frac{\partial}{\partial x}\left(D^{(1)}(c,y)\left(\frac{\partial^2 w^{(1)}}{\partial x^2}(c,y,t)+\mu\frac{\partial^2 w^{(1)}}{\partial y^2}(c,y,t)\right)\right)+2(1-\mu)$$
$$\times\frac{\partial}{\partial y}\left(D^{(1)}(c,y)\frac{\partial^2 w^{(1)}}{\partial x\partial y}(c,y,t)\right)$$
$$=\frac{\partial}{\partial x}\left(D^{(2)}(c,y)\left(\frac{\partial^2 w^{(2)}}{\partial x^2}(c,y,t)+\mu\frac{\partial^2 w^{(2)}}{\partial y^2}(c,y,t)\right)\right)+2(1-\mu)$$
$$\times\frac{\partial}{\partial y}\left(D^{(2)}(c,y)\frac{\partial^2 w^{(2)}}{\partial x\partial y}(c,y,t)\right),\forall y\in[0,b]. \tag{27}$$

Finally we can incorporate the obvious transition condition

$$w^{(1)}(c,y,t)-w^{(2)}(c,y,t)=0,\forall y\in[0,b]. \tag{28}$$

It is well known that for a differential equation of order 4, the boundary conditions containing the function w and derivatives of w of orders not greater than 1, are called *stable* or *geometric*, and those containing derivatives of orders higher than 1, are called *unstable* or *natural*, [19]. In consequence, if $0\leqslant c_r^{(i),j}<\infty, 0\leqslant c_t^{(i),j}<\infty$, the boundary conditions given by Eqs. (22) and (23)and those which correspond to the remaining sides of the plate are all unstable. If this classification is extended to the transition conditions, we conclude that the conditions given by Eqs. (25)–(27) are unstable and Eq. (28) is stable.

The above classification is particularly important when using the Ritz method since we must choose a sequence of functions v_i which constitutes a base in the space of homogeneous essential or geometric boundary conditions. So, in this case, there is no need to subject the functions v_i to the natural boundary and transition conditions.

4. The Ritz and Lagrange multipliers methods

The Eq. (28) ensures the continuity of the transverse deflection along the internal line hinge. Since it is difficult to construct a simple and adequate deflection function which can be applied to the entire plate,and to show the continuity of displacement and the discontinuities of the slope crossing the line hinge,we suggest using the minimization of the energy functional involving subsidiary conditions. The idea is to minimize the mentioned functional over the deflection functions which satisfy the geometrical boundary conditions on the boundary of A and only the continuity requirement on the interface given Eq. (28). One way of dealing with the problem is to force the continuity along the line hinge by means of a suitable Lagrange multiplier [20,22]. This adds a contribution to the energy functional given by:

$$G=G(\lambda,w)=\int_{\Gamma^{(c)}}\lambda(w^{(1)}-w^{(2)})ds$$
$$=\int_0^b\lambda(y)(w^{(1)}-w^{(2)})(c,y)dy, \tag{29}$$

where λ is the Lagrange multiplier.

For free plate vibrations, the displacements of the plate are given by harmonic functions of the time, i.e.

$$w^{(k)}(x,y,t) = W^{(k)}(x,y)\cos\omega t,\ k = 1,2, \tag{30}$$

where ω is the radian frequency of the plate. Substituting Eq. (30) into Eqs. (1) and (3), the maximum kinetic energy $E_{K\max}$ and the maximum strain energy $E_{D\max}$ are obtained. The total energy functional can be written as

$$F_{\max} = E_{K\max} - E_{D\max}.$$

Then the Lagrange multipliers method requires the stationarity of the functional

$$I_G = F_{\max} + G. \tag{31}$$

The approximating functions are chosen assuming that we have two independent subdomains and that these functions verify the corresponding essential boundary conditions. In the application of the Ritz method it is sufficient for the chosen coordinate functions to satisfy the essential or geometric conditions since, as the number of coordinate functions approaches infinity, the natural boundary conditions will be exactly satisfied [18,19]. In the present paper the transverse deflections for $A^{(1)}$ and $A^{(2)}$ are represented by means of the sets of polynomials $\left\{p_i^{(k)}(x)\right\}$ and $\left\{q_j^{(k)}(y)\right\}, k = 1,2,$ as

$$W^{(k)}(x,y) = \sum_{i=1}^{m_k}\sum_{j=1}^{n_k} a_{ij}^{(k)} p_i^{(k)}(x) q_j^{(k)}(y), k = 1,2, \quad x = x/a, y = y/b, \tag{32}$$

where the superscript k denotes the kth subdomain. The coefficients $a_{ij}^{(k)}$ are unknown. The first members $p_1^{(k)}(x)$ and $q_1^{(k)}(y)$ of the sets of polynomials are obtained as the simplest polynomial that satisfies all the geometric boundary conditions of the kth subdomain and are described in Table 1. The polynomials of higher order are obtained as:

$$p_i^{(k)}(x) = p_1^{(k)}(x)x^{i-1}, \quad i = 2,\ldots,m_k. \tag{33}$$

The polynomials set $\left\{q_j^{(k)}(y)\right\}$ is generated by using the same procedure, i.e.

$$q_j^{(k)}(y) = q_1^{(k)}(y)y^{j-1}, \quad j = 2,\ldots,n_k. \tag{34}$$

In this case the Lagrange multiplier is a function which can be represented by a set of polynomials, as:

$$\lambda = \lambda(y) = \sum_{i=1}^{m_3} a_i^{(\lambda)} u_i(y), \tag{35}$$

where $a_i^{(\lambda)}$ are unknown coefficients and $u_i(y) = y^{i-1}$. The application of the Ritz method requires the minimization of the energy functional given by Eq. (31) with respect to each of the unknown coefficients $a_{ij}^{(1)}, a_{ij}^{(2)}$ and $a_i^{(\lambda)}$ by means of the following necessary conditions:

$$\frac{\partial I_G}{\partial a_{ij}^{(1)}} = 0, \quad \frac{\partial I_G}{\partial a_{ij}^{(2)}} = 0, \quad \frac{\partial I_G}{\partial a_i^{(\lambda)}} = 0, \tag{36a, b, c}$$

The application of Eq. (36a,b,c) leads to the following governing eigenvalue equation:

$$([\mathrm{K}] - \Omega^2[\mathrm{M}])\{a\} = \{0\}, \tag{37}$$

where $\Omega = \omega b^2\sqrt{\rho h/D}$ is the non-dimensional frequency parameter. The expressions for the elements of the stiffness matrix $[K]$, the mass matrix $[M]$ and the vector $\{a\}$ are given in the Appendix. For sake of simplicity we adopted $D^{(1)} = D^{(2)} = D$ and $h^{(1)} = h^{(2)} = h$.

The Eq. (37) yields a determinant, whose zeros give the natural frequencies of the mechanical system under study. Back substitution yields the coefficient vectors; and finally substitution of these coefficient vectors into Eq. (32) gives the mode shapes of the plate.

5. Verifications and numerical applications

5.1. Convergence and comparison of eigenvalues and modal shapes

The terminology to be used throughout the remainder of the paper for describing the boundary conditions of the plate considered will now be introduced. The designation CSFS, for example, identifies a plate with the edges 1 clamped, 2 simply supported, 3 free and 4 simply supported (see Fig. 2).

In order to establish the accuracy and applicability of the approach developed and discussed in the previous sections, numerical results were computed for a number of plate problems for which comparison values were available in the literature and also convergence studies have been implemented. Additionally, new numerical results were generated for rectangular plates with an internal line hinge and different boundary conditions. All calculations have been performed taking Poisson's ratio$\mu = 0.3$.

Results of a convergence study of the values of the frequency parameter $\Omega = \omega b^2\sqrt{\rho h/D}$ are presented in Table 2. The first ten values of Ω are presented for a square SSSS plate with an internal line hinge located at two different positions, namely, $\bar{c} = 0.3$ and $\bar{c} = 0.5$ where $\bar{c} = c/a$ (see Appendix). The convergence of the mentioned frequency parameters is studied by gradually increasing the number of polynomial in the approximate functions $W^{(1)}$, $W^{(2)}$ and λ which are respectively given by m_1, n_1, m_2, n_2 and m_3. In this and all the following studies equal numbers of terms have been used, more specifically we adopted $m_1 = n_1 = m_2 = n_2 = m_3 = N$.

It can be observed that the frequency parameters converge monotonically from above as the number of terms increases.

Table 3 gives the first ten values of the frequency parameter $\Omega/\pi^2 = \omega b^2\sqrt{\rho h/D}/\pi^2$ derived by the present method for square plates, together with the values obtained by Xiang and Reddy [15]. The plates considered are simply supported on the two edges parallel to the $x-$ axis with an internal line hinge parallel to the

Table 1
Polynomials bases in the coordinates x and y.

Edge supports		Base polynomials		
$x = 0$ $y = 0$	$x = 1$ $y = 1$	$p_1^{(1)}$	$q_1^{(1)} = q_1^{(2)}$	$p_1^{(2)}$
F	F	1	1	1
S	F	x	y	1
F	C	1	$(y-1)^2$	$(x-1)^2$
S	C	x	$(y-1)^2$	$(x-1)^2$
S	**S**	x	$(y-1)$	$x-1$
C	**C**	x^2	$y^2(y-1)^2$	$(x-1)^2$
C	**S**	x^2	$y^2(y-1)^2$	$x-1$
C	F	x^2	y^2	1
F	**S**	1	$(y-1)$	$x-1$

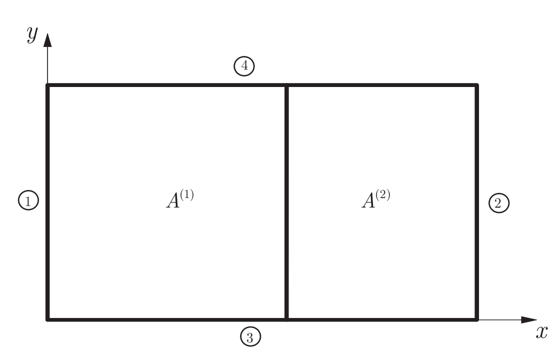

Fig. 2. A rectangular plate with an internal line hinge in a variable position.

Table 2
Convergence study of the first ten values of the frequency parameter $\Omega = \omega b^2\sqrt{\rho h/D}$ for a SSSS square plate with an internal line hinge located at two different positions, $\bar{c} = 0.3, 0.5 \cdot (n_1 = m_1 = n_2 = m_2 = m_3 = N)$.

$\bar{c}$	N	Mode sequence									
		1	2	3	4	5	6	7	8	9	10
0.3	4	16.79617	39.22581	47.60053	72.45622	113.82865	138.13555	141.19845	160.36664	164.73012	199.48865
	5	16.78925	39.11835	47.57079	72.18488	96.74692	98.23627	124.31277	127.03886	155.94957	177.79215
	6	16.78916	39.08628	47.42165	72.01087	96.69062	98.21949	124.20683	126.88881	151.22266	177.79215
	7	16.78915	39.08628	47.42137	72.01029	96.29488	96.80420	122.95390	126.54394	150.69342	172.12537
	8	16.78915	39.08628	47.42073	72.00980	96.29465	96.80387	122.95317	126.54354	150.55578	165.83926
	9	16.78915	39.08628	47.42073	72.00980	96.29286	96.78357	122.93578	126.54224	150.55036	165.83893
0.5	4	16.13895	46.90956	49.35846	76.05570	79.06835	112.54409	137.52645	164.31104	199.26249	209.12610
	5	16.13480	46.88772	49.35764	75.41597	79.06835	97.49083	111.31939	129.53776	166.11499	168.42340
	6	16.13478	46.73884	49.34803	75.28363	78.95725	97.47912	111.02575	129.53336	165.80684	168.42340
	7	16.13478	46.73884	49.34803	75.28363	78.95725	97.47912	111.02575	129.53336	165.80684	168.42340
	8	16.13478	46.73815	49.34802	75.28338	78.95684	96.06096	111.02539	128.32166	164.71055	164.99171
	9	16.13478	46.73815	49.34802	75.28338	78.95684	96.04060	111.02538	128.30494	164.69598	164.99163

Table 3
Comparison study of the first ten values of the frequency parameter $\Omega/\pi^2 = \omega b^2/\pi^2\sqrt{\rho h/D}$ for square plates with an internal line hinge.

Cases	$\bar{c}$		Mode sequence									
			1	2	3	4	5	6	7	8	9	10
SFSS	0.3	Present	1.16669	2.19586	4.14908	5.35664	5.56334	8.95145	9.11707	10.66363	11.71242	14.29167
		Ref.[15]	1.16556	2.18666	4.14343	5.33910	5.54343	8.91145	9.09445	10.62050	11.67830	14.22020
	0.7	Present	1.14571	2.70372	4.09430	4.49394	5.98007	8.53530	9.02618	10.28266	11.03751	13.71081
		Ref. [15]	1.14473	2.69347	4.08803	4.46971	5.96659	8.48238	9.00120	10.25520	11.00540	13.64930
CFSS	0.3	Present	1.28208	2.98105	4.21580	5.84019	6.00232	9.15994	9.39765	10.96627	12.56653	14.70935
		Ref. [15]	1.28051	2.97197	4.20994	5.81851	5.97981	9.13703	9.34764	10.91920	12.52190	14.62370
	0.7	Present	1.24524	3.01334	4.13938	5.33896	6.34725	9.05360	9.12080	11.33219	12.25461	14.57707
		Ref. [15]	1.24394	2.99688	4.13260	5.31502	6.32836	9.02801	9.06092	11.29520	12.21400	14.48030
CSSS	0.3	Present	2.31513	4.60958	5.10475	7.79002	9.99943	10.31290	12.84882	13.44573	16.94566	18.50737
		Ref. [15]	2.31282	4.59602	5.09580	7.75921	9.97150	10.28750	12.79160	13.39820	16.86070	18.42430
	0.7	Present	1.91678	4.91307	4.96438	7.98690	9.92320	11.44474	12.98684	14.23616	16.12256	16.88868
		Ref. [15]	1.91116	4.90107	4.95277	7.95945	9.89318	11.41580	12.93330	14.19240	16.05770	16.80180

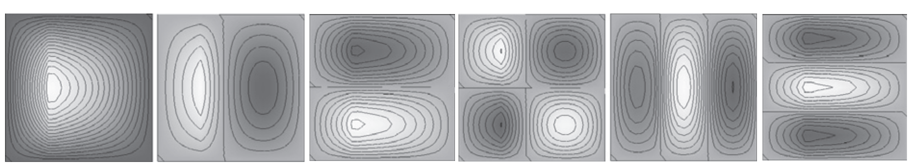

Fig. 3. The first six modal shapes for a SSSS square plate with an internal line hinge located at $\bar{c} = 0.3$.

y-axis. Since the values derived by Xiang and Reddy [15] were based on the first order shear deformation plate theory, for comparison purpose, in the present work, the ratio $h/a = 0.01$ was adopted. It can be observed that the present solutions are in good agreement,from an engineering viewpoint, with the exact solutions of Ref. [15].

A comparison of nodal patterns and modal shapes is also included. Fig. 3 presents the modal shapes of the first six modes for a SSSS square plate with an internal line hinge located at $\bar{c} = 0.3$. These shapes are identical to those obtained by Huang et al. [16].

Another validation of the proposed methodology has been implemented by determining in the case of the fundamental frequency, of a SSFF plate with an internal line hinge located at $\bar{c} = 0.5$, the relative error

$$\varepsilon^{(W)} = (W^{(1)} - W^{(2)})|_{x=\bar{c}}/W_{ref},$$

as a function of the variable y/b, where the $W^{(i)}$ are given by Eq. (32) and W_{ref} is the value of the maximum deflection of the plate given

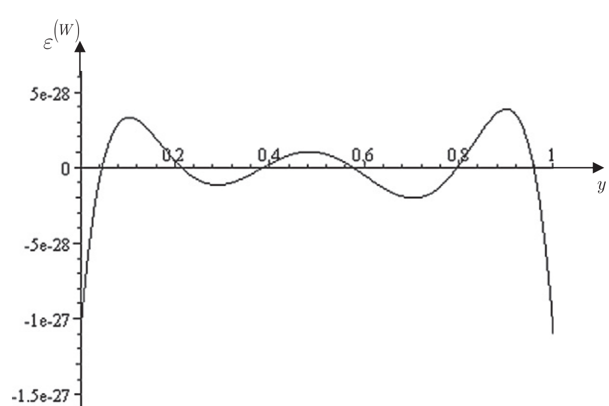

Fig. 4. Relative error $\varepsilon^{(W)} = (W^{(1)} - W^{(2)})|_{x=\bar{c}}/W_{ref}$ as a function of the variable y/b, for the displacements $W^{(1)}$ and $W^{(2)}$ in the internal line hinge.

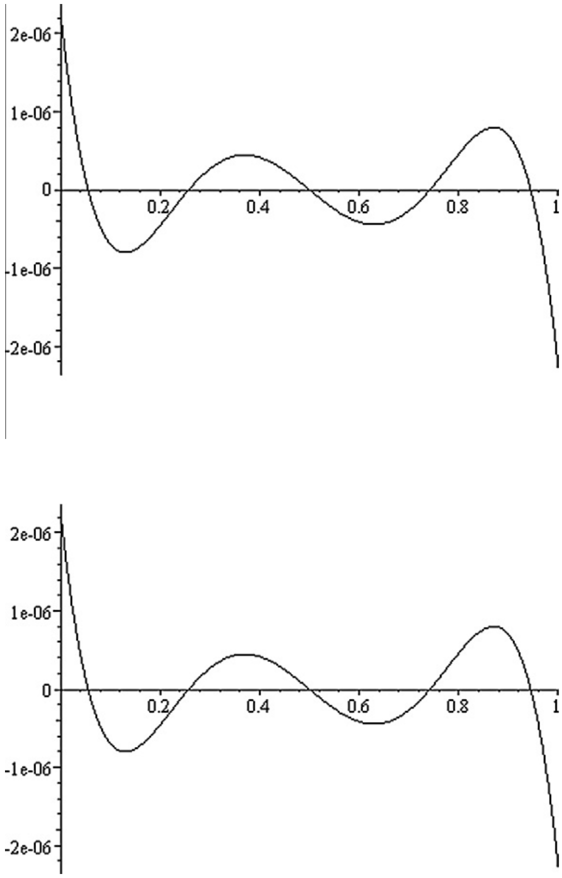

Fig. 5. Variation of the bending moments on the adjacent edges to the line hinge. (a) $\overline{M}_1^{(1)}(\bar{c}, y)$, (b) $\overline{M}_1^{(2)}(\bar{c}, y)$.

by $W_{max} = W^{(1)}(\bar{c}, 0) = 0.2145(10^{-4})$. The results plotted in Fig. 4 represent the relative error $\varepsilon^{(W)}$ for the displacements $W^{(1)}$ and $W^{(2)}$ in the line hinge. It can be observed the continuity of the deflection along the internal line hinge, which demonstrates that the geometric constraint 28 is satisfied.

$\bar{c}$	Mode 1	Mode 2	Mode 3
0.1	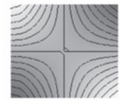 $\Omega_1 = 13.18792$	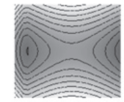 $\Omega_2 = 20.71540$	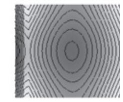 $\Omega_3 = 26.94847$
0.3	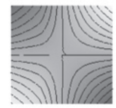 $\Omega_1 = 13.24793$	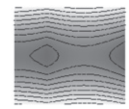 $\Omega_2 = 21.36147$	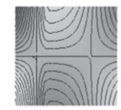 $\Omega_3 = 30.42241$
0.5	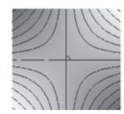 $\Omega_1 = 13.46822$	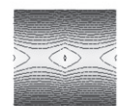 $\Omega_2 = 21.46337$	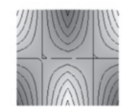 $\Omega_3 = 26.57505$

Fig. 7. The first three values of the frequency parameter $\Omega = \omega b^2 \sqrt{\rho h / D}$ and contour lines of a FFFF square plate with an internal line hinge located at different positions.

Finally, to validate the solutions obtained for a hinged massless joint which provides zero bending moment on the adjacent edges to the line hinge, the variation of $\overline{M}_1^{(1)}(\bar{c}, y)$ and $\overline{M}_1^{(2)}(\bar{c}, y)$ are shown in Fig. 5a and b. The parameters $\overline{M}_1^{(k)}$ are given by $\overline{M}_1^{(k)} = M_1^{(k)} a^2 / D$ with $M_1^{(k)}$ given by Eq. (15a). All these figures clearly illustrate that the bending moments on the line $\Gamma^{(c)}$ practically take the value zero and that the deflection functions satisfy the transition condition (28).

5.2. New numerical results

The advantage of the approach developed here can be exploited together useful and rapid information about the effects of the

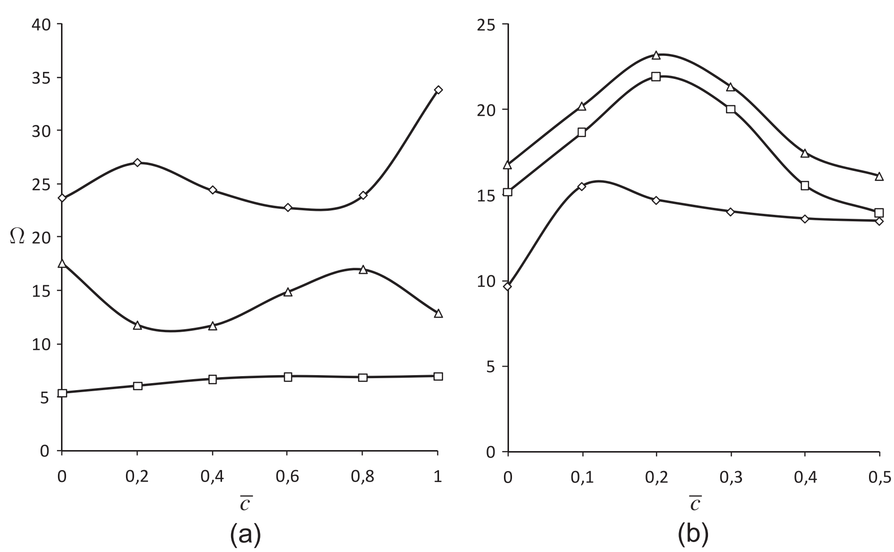

Fig. 6. First value of the frequency parameter $\Omega = \omega b^2 \sqrt{\rho h / D}$ versus the location parameter of the internal line hinge $\bar{c}$ for: (a) asymmetric boundary conditions: □, CFCF plates; △, SCCF plates; ◇, CSCS plates and (b) symmetric boundary conditions: □, CCFF plates; △, CCSF plates; ◇, SSFF plates.

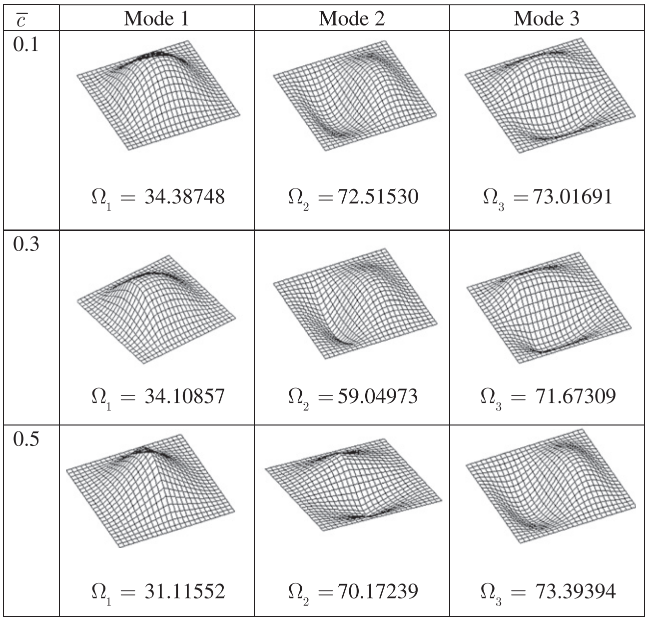

Fig. 8. The first three values of the frequency parameter $\Omega = \omega b^2\sqrt{\rho h/D}$ and modal shapes of a CCCC square plate with an internal line hinge located at different positions.

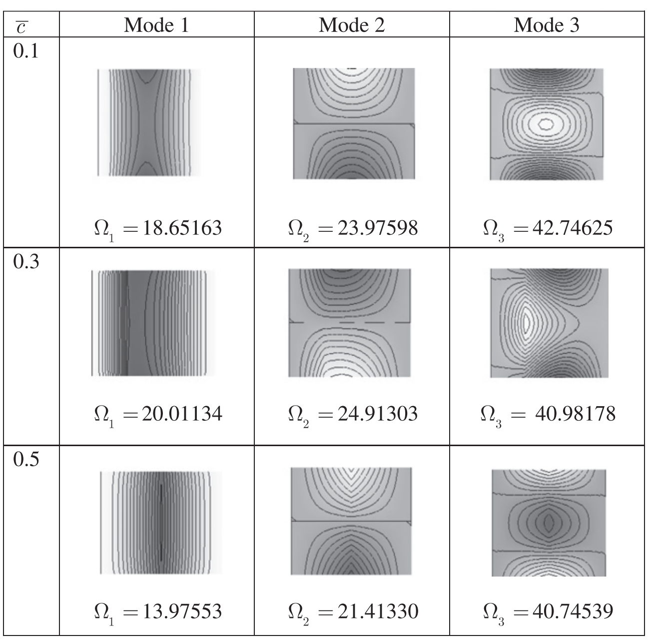

Fig. 9. The first three values of the frequency parameter $\Omega = \omega b^2\sqrt{\rho h/D}$ and contour lines of a CCFF square plate with an internal line hinge located at different positions.

geometry and boundary conditions on the natural frequencies of the plate with a line hinge when two parallel edges are not simply supported. As an example, the Fig. 6 shows the variations of the first value of the frequency parameter Ω with respect to the hinge location for three square plates with asymmetric boundary conditions at the edges parallel to the line hinge (see Fig. 6a) and three square plates with symmetric boundary conditions (see Fig. 6b). These figures clearly illustrate how the location of the internal line hinge affects the frequency parameters of the plates.

Figs. 7–9 present the first three values of the frequency parameter $\Omega = \omega b^2\sqrt{\rho h/D}$ and the associated contour lines or three-dimensional mode shape for FFFF, CCCC and CCFF square plates with an internal line hinge located at three different points. It can be observed that the line hinge presence introduces significant deformations and discontinuity of the slope along this line.

Table 4
The first five values of the frequency parameter $\Omega = \omega b^2\sqrt{\rho h/D}$ and nodal patterns for a square plate with four edges elastically restrained against rotation $\left(R = R_i^{(1)} = R_i^{(2)}, i = 1,2,3\right)$ and translation $\left(T = T_i^{(1)} = T_i^{(2)}, i = 1,2,3\right)$. The line hinge is located at $\bar{c} = 0.5$.

R	T	Ω_1	Ω_2	Ω_3	Ω_4	Ω_5
∞	1	1.9955	9.9287	10.1687	19.9407	22.4840
	10	6.1824	12.2568	12.5216	21.6615	23.4725
	100	16.3072	24.6268	25.2947	32.3352	33.8958
	1000	27.0384	52.5708	54.6714	67.8418	72.6893
1000	1	1.9954	9.9111	10.1492	19.9083	22.4264
	10	6.1809	12.2454	12.5087	21.6353	23.4203
	100	16.2802	24.6226	25.291	32.3188	3.8934
	1000	26.9517	52.4640	54.5642	67.7696	72.5875
100	1	1.950	9.7568	9.979	1.6317	21.271
	10	6.1674	12.1463	12.3969	21.4116	22.9694
	100	16.0470	24.5869	25.2642	32.1792	33.8729
	1000	26.2264	51.5837	53.6812	67.1799	71.7601
10	1	1.9908	8.595	8.689	17.869	18.211
	10	6.0442	11.4025	11.5741	19.7391	19.9776
	100	14.3883	24.3552	25.0847	31.2795	33.7518
	1000	21.9852	46.9218	49.0536	64.2123	67.7309

Table 4 depicts the first five values of the frequency parameter $\Omega = \omega b^2\sqrt{\rho h/D}$ for a square plate with four edges elastically restrained against rotation $\left(R_i^{(1)} = R_i^{(2)} = R, i = 1,2,3\right)$ and translation $\left(T_i^{(1)} = T_i^{(2)} = T, i = 1,2,3\right)$. The internal line hinge is located at $\bar{c} = 0.5$. This table shows the effect of both restraints parameters applied simultaneously. It can be observed that the rotational restrain parameter R has little effect on the frequency coefficient Ω but there is a large increase of its values when the translational restraint T is increased.

Table 5 depicts the first ten values of the frequency parameter $\Omega = \omega b^2\sqrt{\rho h/D}$ for CFFF, CSFF, FFFF and CCCC rectangular plates. The plate aspect ratio b/a is taken equal to 1/2 and 1/3 and the internal line hinge is located at different positions. It is clear from the results presented in the mentioned table that the frequency parameters are affected by the line hinge location. It can be seen that the effect over the frequencies is highly sensitive to the boundary conditions of the plates.

6. Conclusions

This paper presents the formulation of an analytical model for the dynamic behavior of rectangular isotropic plates, with an arbitrarily located internal line hinge and boundaries elastically restrained against rotation and translation. The equations of motion and its associated boundary and transition conditions were rigorously derived using Hamilton's principle. An approach to the solution of the natural vibration problems, of the mentioned plates by a direct variational method, has been presented. A simple, computationally efficient and accurate algorithm has been developed for the determination of frequencies and modal shapes of natural vibrations. The approach is based on a combination of the Ritz method and the Lagrange multipliers method. Sets of parametric studies have been performed to show the influence of the line hinge and its location on the vibration behavior. Finally, it is important to point out that the method presented can be easily modified to be applied to static deflection problems and buckling analysis. On the other hand, the method can be easily generalized for analyzing anisotropic plates.

Table 5
The first ten values of the frequency parameter $\Omega = \omega b^2\sqrt{\rho h/D}$ for rectangular plates with different boundary conditions and with an internal line hinge located at different positions.

Cases	b/a	$\bar{c}$	Mode Sequence									
			1	2	3	4	5	6	7	8	9	10
CFFF	1/2	1/3	3.70039	4.23226	10.97744	11.37595	21.33792	23.25375	28.61012	31.29841	38.14117	42.46425
		1/2	2.43433	3.68618	11.36009	15.03883	20.43894	22.85671	24.53022	30.95284	33.17192	44.31261
		2/3	1.58471	3.67354	10.39674	11.95138	20.34555	22.69341	28.98979	31.55609	37.10921	42.90530
	1/3	1/3	2.34785	4.88296	7.19868	12.84421	12.89246	18.52094	20.70305	22.50846	26.33017	27.62041
		1/2	1.07581	2.34520	6.66945	7.23479	9.53061	13.18810	19.26823	21.48576	22.89995	25.25240
		2/3	0.70019	2.34304	4.60278	7.36998	12.61387	12.86907	18.11722	20.15549	22.95472	26.51224
CSFF	1/2	1/3	3.51554	7.68729	8.21567	16.48237	23.84415	26.59440	31.71965	36.99155	40.60754	48.24853
		1/2	2.23689	7.49831	11.37617	18.02897	19.13922	26.52227	28.43581	38.10617	42.29858	50.26304
		2/3	1.50140	7.51825	10.05115	17.09667	24.69953	26.37498	32.24363	34.21046	37.75569	43.97461
	1/3	1/3	1.55403	3.63483	4.77971	10.02977	10.58499	17.30863	17.76210	23.54265	25.20263	25.25155
		1/2	0.98842	4.74981	5.02579	8.52647	10.42137	16.30680	18.64217	23.50794	25.77783	26.00811
		2/3	0.66334	4.44817	4.75985	10.16473	10.99140	14.99632	17.43077	23.99252	24.07921	27.54311
FFFF	1/2	1/3	6.60424	10.34880	14.14352	21.81490	22.58888	25.46545	28.99325	35.84744	39.42025	42.94824
		1/2	6.64373	13.46824	14.90154	19.59627	24.27068	25.37579	26.00085	34.80135	34.80135	48.45422
	1/3	1/3	4.36459	4.60037	9.14525	12.76021	14.21635	18.09963	22.02086	22.13062	24.26271	28.57216
		1/2	4.37560	6.61661	8.93139	9.51710	15.07240	20.59894	21.31491	22.18323	24.35011	25.65404
CCCC	1/2	1/3	24.13002	30.04194	44.54295	58.10117	63.41626	69.97441	78.85972	83.21104	97.628841	15.85963
		1/2	23.92702	31.82602	40.00247	63.23209	63.33094	71.07644	76.71410	80.58045	100.792821	16.41630
	1/3	1/3	23.00374	25.36346	30.69778	36.44913	45.04034	60.16477	62.29117	65.08278	70.42977	71.21769
		1/2	22.93536	25.85940	29.38919	38.09392	44.33273	60.32777	62.19775	65.50936	68.90407	69.56422

Acknowledgment

The present investigation has been sponsored by the CONICET Project PIP 2011-2013 D 753.

Appendix A. Coefficients of Eq. (37).

$$[K] = \begin{bmatrix} [K^{(1,1)}] & [0] & [K^{(1\lambda)}] \\ & [K^{(2,2)}] & [K^{(2,\lambda)}] \\ \text{sim.} & & [0] \end{bmatrix}, [M] = \begin{bmatrix} [M^{(1,1)}] & [0] & [0] \\ & [M^{(2,2)}] & [0] \\ \text{sim.} & & [0] \end{bmatrix}$$

and $\{a\} = \left\{ a_{ij}^{(1)}, a_{ij}^{(2)}, a_i^{(\lambda)} \right\}^T$,
where

$$K_{ijmn}^{(k,k)} = r^4 P_{im}^{(2,2,k)} Q_{jn}^{(0,0,k)} + P_{im}^{(0,0,k)} Q_{jn}^{(2,2,k)} + 2r^2(1-\mu) P_{im}^{(1,1,k)} Q_{jn}^{(1,1,k)} + r^2\mu\left(P_{im}^{(2,0,k)} Q_{jn}^{(0,2,k)} + P_{im}^{(0,2,k)} Q_{jn}^{(2,0,k)}\right) + \sum_{s=1}^{3} B_s^{(k)} \left(Rx_{im}^{(k)}\right)_s \left(Ry_{jn}^{(k)}\right)_s + \sum_{s=1}^{3} C_s^{(k)} \left(Tx_{im}^{(k)}\right)_s \left(Ty_{jn}^{(k)}\right)_s$$

$$K_{ijm}^{(k,\lambda)} = r^4 T_m \left(F_{ij}^{(0,0,k)}\right)$$

$$M_{ijmn}^{(k,k)} = P_{im}^{(0,0,k)} Q_{jn}^{(0,0,k)}, \quad k = 1,2.$$

where

$$P_{im}^{(r,s,1)} = \int_0^{\bar{c}} \frac{\partial^r p_i^{(1)}(x)}{\partial x^r} \frac{\partial^s p_m^{(1)}(x)}{\partial x^s} dx, \quad P_{im}^{(r,s,2)} = \int_{\bar{c}}^1 \frac{\partial^r p_i^{(2)}(x)}{\partial x^r} \frac{\partial^s p_m^{(2)}(x)}{\partial x^s} dx,$$

$$Q_{jn}^{(r,s,k)} = \int_0^1 \frac{\partial^r q_j^{(k)}(y)}{\partial y^r} \frac{\partial^s q_n^{(k)}(y)}{\partial y^s} dy,$$

$$\left(Rx_{im}^{(1)}\right)_1 = \frac{\partial p_i^{(1)}(0)}{\partial x} \frac{\partial p_m^{(1)}(0)}{\partial x}, \quad \left(Ry_{jn}^{(1)}\right)_1 = Q_{jn}^{(0,0,1)},$$

$$\left(Rx_{im}^{(2)}\right)_1 = \frac{\partial p_i^{(2)}(1)}{\partial x} \frac{\partial p_m^{(2)}(1)}{\partial x}, \quad \left(Ry_{jn}^{(2)}\right)_1 = Q_{jn}^{(0,0,2)},$$

$$\left(Rx_{im}^{(k)}\right)_2 = P_{im}^{(0,0,k)}, \quad \left(Ry_{jn}^{(k)}\right)_2 = \frac{\partial q_j^{(k)}(0)}{\partial y} \frac{\partial q_n^{(k)}(0)}{\partial y},$$

$$\left(Rx_{im}^{(k)}\right)_3 = P_{im}^{(0,0,k)}, \quad \left(Ry_{jn}^{(k)}\right)_2 = \frac{\partial q_j^{(k)}(1)}{\partial y} \frac{\partial q_n^{(k)}(1)}{\partial y},$$

$$\left(Tx_{im}^{(1)}\right)_1 = p_i^{(1)}(0) p_m^{(1)}(0), \quad \left(Ty_{jn}^{(1)}\right)_1 = Q_{jn}^{(0,0,1)},$$

$$\left(Tx_{im}^{(2)}\right)_1 = p_i^{(2)}(1) p_m^{(2)}(1), \quad \left(Ty_{jn}^{(2)}\right)_1 = Q_{jn}^{(0,0,2)},$$

$$\left(Tx_{im}^{(k)}\right)_2 = P_{im}^{(0,0,k)}, \quad \left(Ty_{jn}^{(k)}\right)_2 = q_j^{(k)}(0) q_n^{(k)}(0),$$

$$\left(Tx_{im}^{(k)}\right)_3 = P_{im}^{(0,0,k)}, \quad \left(Ty_{jn}^{(k)}\right)_3 = q_j^{(k)}(1) q_n^{(k)}(1),$$

$$B_1^{(k)} = R_2^{(k)} r^4, \quad R_2^{(k)} = \frac{c_r^{(k),2} a}{D}, \quad C_1^{(k)} = T_2^{(k)} r^4, \quad T_2^{(k)} = \frac{c_t^{(k),2} a^3}{D},$$

$$B_2^{(1)} = R_3^{(1)}, \quad R_3^{(1)} = \frac{c_r^{(1),3} b}{D}, \quad C_2^{(1)} = T_3^{(1)}, \quad T_3^{(1)} = \frac{c_t^{(1),3} b^3}{D},$$

$$B_2^{(2)} = R_1^{(2)}, \quad R_1^{(2)} = \frac{c_r^{(2),1} b}{D}, \quad C_2^{(2)} = T_1^{(2)}, \quad T_1^{(2)} = \frac{c_t^{(2),1} b^3}{D},$$

$$B_3^{(1)} = R_1^{(1)}, \quad R_1^{(1)} = \frac{c_r^{(1),1} b}{D}, \quad C_3^{(1)} = T_1^{(1)}, \quad T_1^{(1)} = \frac{c_t^{(1),1} b^3}{D},$$

$$B_3^{(2)} = R_3^{(2)}, \quad R_3^{(2)} = \frac{c_r^{(2),3} b}{D}, \quad C_3^{(2)} = T_3^{(2)}, \quad T_3^{(2)} = \frac{c_t^{(2),3} b^3}{D},$$

$$F_{ij}^{(r,s,k)} = \frac{\partial^r p_i^{(k)}}{\partial x^r}(\bar{c})() \int_0^1 \frac{\partial^s q_j^{(k)}(y)}{\partial y^s} dy, \quad k = 1,2. \quad T_m = \int_0^1 u_m(y) dy,$$

where $x = x/a$, $y = y/b, r = b/a$, $\bar{c} = c/a, a$ and b are the length sides of the plate.

References

[1] Leissa AW. Vibration of plates. NASA SP-160. Washington DC. NASA; 1969.
[2] Blevins RD. Formulas for natural frequency and mode shape. Malabar, Florida: Krieger Publishing Company; 1993.
[3] Gorman DJ. Free vibration analysis of plates. New York: Elsevier; 1982.
[4] Timoshenko S, Woinowsky-Krieger S. Theory of plates and shells. New York: McGraw-Hill; 1959.
[5] Reddy JN. Mechanics of laminated composite plates and shells: theory and analysis. 2nd ed. Boca Raton, Florida: CRC Press; 2004.
[6] Leissa AW. The free vibration of rectangular plates. J Sound Vib 1973;31:257–93.
[7] Leissa AW. Recent research in plate vibrations, 1973–1976: complicating effects. Shock Vib Dig 1978;10(12):21–35.
[8] Fan SC, Cheung YK. Flexural free vibrations of rectangular plates with complex support conditions. J Sound Vib 1984;31:81–94.
[9] Kim CS, Dickinson SM. The flexural vibration of rectangular plates with point support. J Sound Vib 1987;117:249–61.
[10] Liew KM, Liu FL. Effects of arbitrarily distributed elastic point constraints on vibrational behaviour of rectangular plates. J Sound Vib 1994;174:23–36.
[11] Zhou D. Vibration point-supported rectangular plates with variable thickness using a set of static tapered beam functions. Int J Mech Sci 2002;44:149–64.
[12] Kim CS, Dickinson SM. The flexural vibration of line supported rectangular plate systems. J Sound Vib 1987;114:129–42.
[13] Zhou D, Cheung YK. Free vibration of line supported rectangular plates using a set of static beam functions. J Sound Vib 1999;223:231–45.
[14] Xiang Y, Zhao YB, Wei GW. Levy solutions for vibration of multi-span rectangular plates. Int J Mech Sci 2002;44:1195–218.
[15] Xiang Y, Reddy JN. Natural vibration of rectangular plates with an internal line hinge using the first order shear deformation plate theory. J Sound Vib 2003;263:285–97.
[16] Huang M, Ma XQ, Sakiyama T, Matsuda H, Morita C. Natural vibration study on rectangular plates with a line hinge and various boundary conditions. J Sound Vib 2009;322:227–40.
[17] Lin TR, Pan J, Mechefske CK. The effect of off-neutral axis excitation on the vibration response of finite ribbed-plates. J Vib Acoust 2009;131(1). 011011, 1-11.
[18] Mikhlin S. Variational methods of mathematical physics. New York: Mac Millan Co.; 1964.
[19] Rektorys K. Variational methods in mathematics. Science and engineering. Dordrecht: Reidel Co.; 1980.
[20] Reddy JN. Applied functional analysis and variational methods in engineering. New York: McGraw Hill; 1986.
[21] Gelfand IM, Fomin SV. Calculus of variations. New Jersey: Prentice-Hall Inc.; 1963.
[22] Luemberger D. Optimization by vector space methods. New York: J. Wiley; 1969.
[23] Troutman JL. Variational calculus and optimal control. New York: Springer-Verlag; 1996.